



Fabrication of chitosan-alginate-polyvinylpyrrolidone for efficient removal of Cr(VI) from wastewater in experiment and adsorption mechanism

Amru Daulay¹ · David Candra Birawidha¹ · Singgih Prabowo¹ · Evi Dwi Yanti¹ · Lukman Hakim Nasution¹ · Yassaroh Yassaroh² · Lukmanul Hakim Samada³

Received: 19 June 2024 / Revised: 4 July 2024 / Accepted: 4 July 2024

© The Author(s), under exclusive licence to Springer Science+Business Media, LLC, part of Springer Nature 2024

Abstract

This study synthesized chitosan-alginate-polyvinylpyrrolidone and applied it for Cr(VI) removal. Characterization was carried out using FTIR, TGA, N₂ adsorption, ¹H NMR, and FE-SEM. FTIR spectra show peaks at 1415 cm⁻¹, 1323 cm⁻¹, 1029 cm⁻¹, and 448 cm⁻¹, which are COO, C-N, C-O, and N-C=O groups. The surface area of CsAgPVP was 20.42 m²/g. The pore size of CsAgPVP was 5.36 nm. Field emission shows the C, O, N, and Na. The optimum conditions CsAgPVP for adsorption Cr(VI) were 50 ppm, 360 min, and pH 4. It uses adsorption isotherm and kinetic to show the Langmuir model and pseudo-second-order. The CsAgPVP adsorption process is assumed homogeneous and considered as chemisorption. Adsorption capacity shows 208.67 mg/g. It uses a regeneration study of removal percentage up to 90% in the fourth cycle. The removal percentage in real sample mine wastewater and waste acid laboratories was 80% and 72%.

Keywords Chitosan · Alginate · Polyvinylpyrrolidone · Cr(VI) · Wastewater treatment

1 Introduction

Hexavalent chromium [Cr(VI)] is a heavy metal that adversely affects humans and the environment. These heavy metals enable to contaminate water sources. The impact can harm the water ecosystem and can enter the food chain. Health problems such as organ damage, poor child development, neurological problems, and cancer can be raised from exposure to these heavy metals [1, 2]. Developing appropriate waste management techniques and efficient management procedures are essential to reduce heavy metals in the water.

Cr(VI) can be found in nature as a chromite ore. They are widely employed in leather tanning, electroplating, the textile industry, and chromite ore processing [3, 4]. These metals are known as dangerous threats to the environment and humans. Furthermore, Cr(VI) has very high toxicity and carcinogenic potential. The World Health Organization (WHO) recommended a minimum Cr(VI) concentration in drinking water of 0.05 mg/L [5, 6].

Coagulation, chemical precipitation, ion exchange, and reverse osmosis treat heavy metal pollution [7]. However, these methods are not effective in high-discharge effluents. Among various treatment methods, adsorption is efficient due to its simple operation, high efficiency, and ability to remove chemical compounds [8]. Adsorption methods are exploited due to their remediation process, which is technically reliable and inexpensive. Adsorption methods using complex materials have been investigated [9]. Various adsorbents have been investigated for Cr(VI) adsorption from aqueous media [10]. Some common low-cost adsorbents involved chitosan, sodium alginate, and polyvinylpyrrolidone. Chitosan is a cationic polysaccharide biopolymer that has many amine and hydroxyl groups. Chitosan has a protonated amino function. Chitosan is the second most

✉ Amru Daulay
amru006@brin.go.id

¹ Research Center for Mining Technology, National Research and Innovation Agency (BRIN), Jl. Ir. Sutami, Km. 15, Tanjung Bintang, South Lampung, Lampung Province, Indonesia

² Research Center for Polymer Technology, National Research and Innovation Agency (BRIN), KST BJ. Habibie, Puspipstek Area Building 460, Tangerang Selatan 15314, Indonesia

³ School of Chemistry, University of Birmingham, Birmingham B15 2TT, UK

abundant biopolymer in nature and is widely used as a polymer solution to modify membrane surfaces and improve anti-foul and hydrophilic properties [11]. It is a hydrophilic, inexpensive, non-toxic, and biodegradable agent. Chitosan chains are utilized to bind metal anions. The presence of amines enables them to enhance their binding ability. It makes chitosan graftable involving organic functions or molecules. It is possible to modify the material affinity by grafting chitosans according to specific species or conditions [12]. Sodium alginate consists of D-mannuronate and L-guluronate with random distribution. Sodium alginate is also a material used for wastewater management. The specific surface area, porosity, and number of active sites of alginate can be increased by modification [13]. Polyvinylpyrrolidone (PVP) is a polymer with low cost, good capacity, prominent biological compatibility, and good environmental stability. PVP contains amino groups that bind to anions such as CrO_4^{2-} and HCrO_4^- [14].

The novelty of this study was to fabricate two biopolymers based on chitosan and alginate with modified polymer PVP. PVP was chosen because it contains amino groups that can bind to other anions. The new material will produce adsorbents with great potential in removing Cr(IV) from wastewater. This study also used a real sample in the mine wastewater and waste acid laboratory.

2 Materials and methods

2.1 Materials

Mine wastewater and waste acid laboratory samples were obtained from Indonesia. Acetic acid (CH_3COOH 99 wt%), chromium trioxide (CrO_3 99 wt%), sodium hydroxide (NaOH 98 wt%), hydrochloric acid (HCl 37 wt%), chitosan, sodium alginate, and polyvinylpyrrolidone (PVP) were purchased from Sigma-Aldrich. Distilled water was purchased from local chemical distributors in Indonesia. All the chemical reagents were utilized without any additional purification.

2.2 Fabrication of chitosan-alginate-polyvinylpyrrolidone

Prepare chitosan of 2 g, sodium alginate of 10 g, and PVP of 0.2 g. The three materials were mixed and dissolved into 90 mL CH_3COOH while stirring at room temperature at 200 rpm for 3 h. filtering was done, and the solid fraction was obtained after 3 h. The solid fraction was washed with distilled water until pH 7. The solid fraction was heated at 80 °C for 6 h. This sample was named CsAgPVP.

2.3 Characterization

Fourier-transform infrared spectroscopy (FTIR, INVENIO FT-IR Spectrometer) spectra were recorded using a PerkinElmer spectrometer in the $4000\text{ cm}^{-1} - 400\text{ cm}^{-1}$ range at the ambient temperature. Thermal gravimetric analysis (TGA) was performed under an inert atmosphere of N_2 at a heating rate of 10 °C min^{-1} , from room temperature to 800 °C, on a PerkinElmer TGA 400. Nuclear magnetic resonance ($^1\text{H NMR}$, Nanalysis Ready 60 Pro. Nitrogen adsorption and desorption isotherms were determined by nitrogen physisorption at 77 K with a degassing temperature of 565 K for 1 h on Quantachrome (Quantachrome TouchWin v1.11) instruments. Field emission-scanning electron microscope (FE-SEM, Thermo Fisher Quattro S) operates at 20 kV to investigate the morphology.

2.4 Adsorption test

Adsorption tests were conducted at 25 °C with a stirring speed of 200 rpm. The weight of the adsorbent used is 50 mg in 50 mL of Cr(VI) solution. First, a 1000 ppm Cr(VI) as parent solution was prepared by dissolving 3 g CrO_3 in 1000 mL distilled water. The effect of concentration by the adsorption process was carried out with various concentrations: 50 ppm, 100 ppm, 150 ppm, 200 ppm, 250 ppm, and 300 ppm. The effect of time on the adsorption process was carried out at various times: 60 min, 120 min, 180 min, 240 min, 300 min, and 360 min with temperatures 298–328 K. The effect of pH on the adsorption process was employed at 1, 2, 3, 4, 5, 6, 7, and 8. The pH solution was added with 0.1 M HCl and 1 M NaOH . The solids were separated using filter paper after stirring. To determine the concentration of Cr(VI) using an atomic absorption spectrometer (AAS, Shimadzu AA-7000). Adsorption tests were also conducted with real samples using mine wastewater and waste acid laboratory in Indonesia. Samples were taken at rapid intervals and filtered by filter paper.

3 Result and discussion

3.1 Characterization

In the formation reaction, CsAgPVP will form a group of -COO- groups from alginate when chitosan is mixed with PVP. It happens in the CH_3COOH solution. The mixture will produce molecules that react in each polymer chain through ionic interactions between chitosan as a positive ion and alginate as a negative ion. Hydrogen bonding also occurs on the -OH group of chitosan and the CO group of PVP. There is also a formation between the -COO- of alginate and the

Fig. 1 Characterization chitosan, alginate, PVP, and CsAgPVP of (a) FTIR spectra, (b) TGA graph, (c) N₂ adsorption-desorption isotherm, and (d) pore size distribution curves

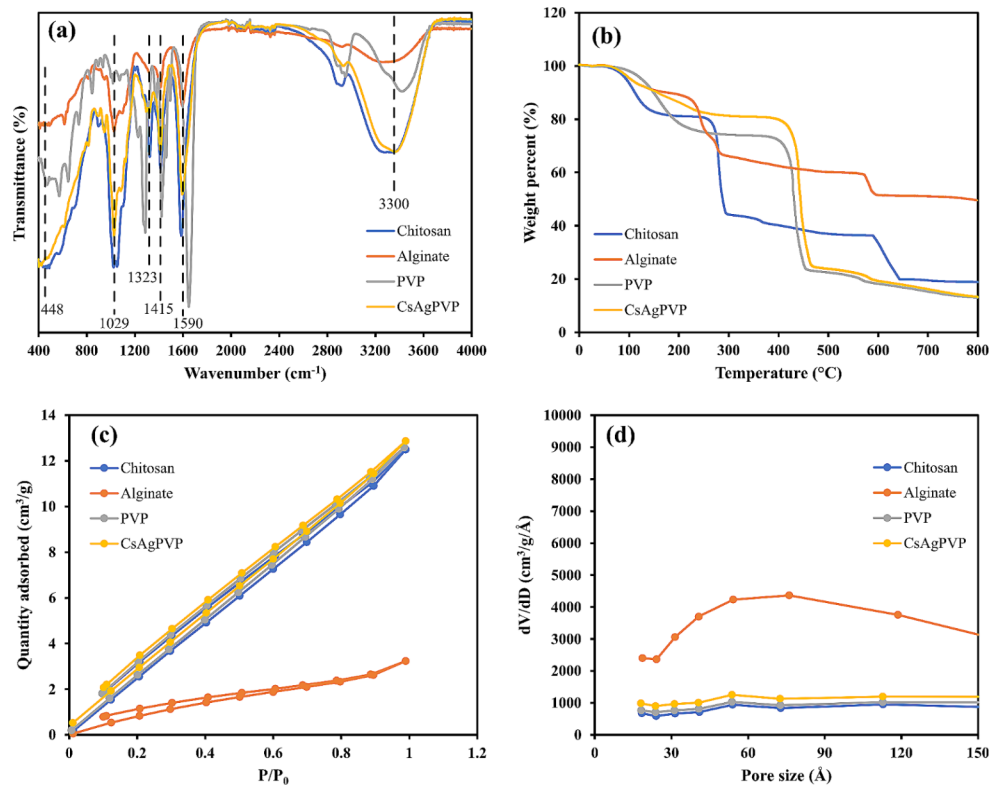


Table 1 Physical properties of chitosan, alginate, PVP, and CsAgPVP

Samples	BET surface area (m ² /g)	Pore volume (cm ³ /g)	Pore size (nm)
Chitosan	20.33	0.019	5.38
Alginate	5.13	0.005	7.61
PVP	20.73	0.019	5.37
CsAgPVP	20.42	0.019	5.36

NH₂ of chitosan. Chitosan will crosslink to form the Schiff base with amino and carbonyl groups [15].

FTIR spectra can be seen in Fig. 1a. The CsAgPVP shows bonding between CH₂ and N-C=O bending at the adsorption peak of 448 cm⁻¹ [16, 17]. The adsorption at 1415 cm⁻¹ shows the simulated stretching vibration of COO. The adsorption at 1323 cm⁻¹ shows the stretching vibration in the C-N group. The adsorption peak at 1029 cm⁻¹ also shows C-O stretching. The stretching of the OH group with N-H stretch can be seen in the adsorption peak at 3300 cm⁻¹. The TGA graph can be seen in Fig. 1b. The first mass loss of CsAgPVP occurred at 100 °C but did not reduce much. The mass is still at the 93% stage. The second mass reduction was at 400 °C and continued to reduce up to 450%. The remaining mass is around 25%. The temperature of 800 °C caused a reduction to the final mass of 20%. The mass of CsAgPVP loss is similar to that of PVP but with an increase. The combination of chitosan, alginate, and PVP causes an increase in temperature resistance. The

mixed materials will improve the physical properties of one of them at high temperatures [18, 19]. N₂ adsorption characterization using *t*-plot can be seen in Fig. S1. N₂ adsorption characterization for using BET surface area (Fig. 1c) and BJH pore volume (Fig. 1d). Physical properties of chitosan, alginate, PVP, and CsAgPVP result of N₂ adsorption can be seen in Table 1. The surface area of chitosan, alginate, PVP, and CsAgPVP are 20.33 m²/g, 5.13 m²/g, 20.73 m²/g, and 20.42 m²/g. Chitosan, alginate, PVP, and CsAgPVP pore sizes are 5.38 nm, 7.61 nm, 5.37 nm, and 5.36 nm. The formed CsAgPVP has a high surface area and pore size.

The ¹H NMR spectra can be seen in Fig. 2. Chitosan and alginate have good solubility [20]. It makes grafted chitosan very possible. PVP and alginate grafted on the synthesized chitosan can be through a condensation reaction followed by the formation of the grafted polymer [21, 22]. CsAgPVP was formed by crosslinking alginate and PVP. The spectra of CsAgPVP showed a new peak at 2.19 ppm derived from PVP.

FE-SEM images can be seen in Fig. 3. The morphology of chitosan is like elongated fine threads. The morphology of alginate is like that of fine dust clumps with a small surface area. PVP morphology shows fine spherical chunks. The combined morphological forms of chitosan, alginate, and PVP are seen in CsAgPVP. The morphology of CsAgPVP has small spheres incorporated on the surface area that look like fine threads and contain small clumps inside. It indicates that CsAgPVP has been formed.

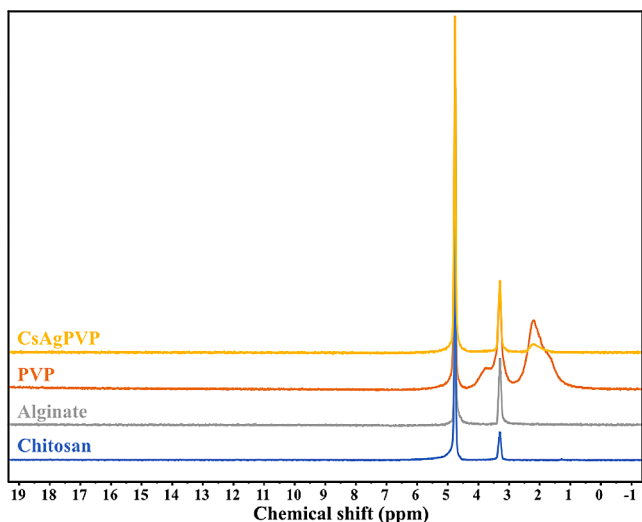


Fig. 2 ¹H NMR spectra of the chitosan, alginate, PVP, and CsAgPVP

3.2 Adsorption study

The adsorption effect of CsAgPVP on Cr(VI) using different concentrations can be seen in Fig. S2. Cr(VI) adsorption using adsorbent CsAgPVP showed the highest removal percentage at 50 ppm. The higher the concentration of Cr(VI), the lower the adsorption ability. The higher the Cr(VI) concentration, the more concentrated the solution. The density will strengthen the bond between Cr(VI) and water, making it difficult for the adsorbent to absorb [23].

An adsorption study was carried out using variation contact time using a Cr(VI) concentration of 50 ppm. The

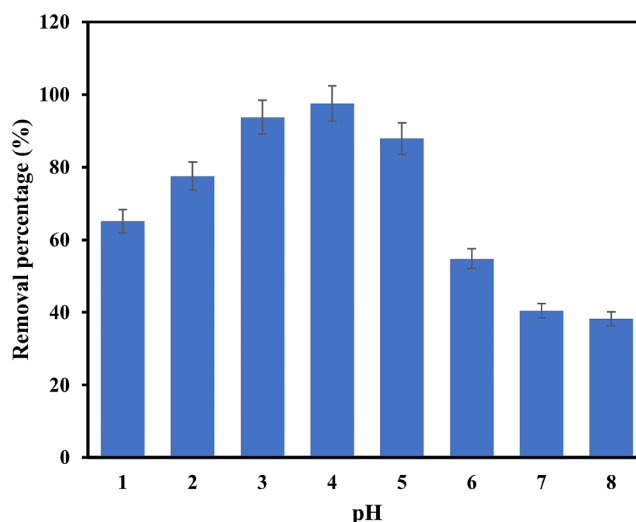


Fig. 4 Effect of pH on the adsorption of CsAgPVP at an adsorption Cr(VI) with experiment condition: contact time=60 min; adsorbent dose=1 g/L; concentration=50 ppm

adsorption effect of CsAgPVP on Cr(VI) using different contact times can be seen in Fig. S3. The variation in contact time in the adsorption study shows that the highest removal percentage is at 360 min. It shows that the longer the contact time between CsAgPVP adsorbent and Cr(VI), the more effective it will be. In the adsorption process, it will take time for the adsorbent to work. The longer the time in the adsorption process, the more effective it will be. Adding a long time will maximize the adsorbent's performance [24].

The effect of pH on the performance of CsAgPVP in Cr(VI) adsorption can be seen in Fig. 4. The pH variation

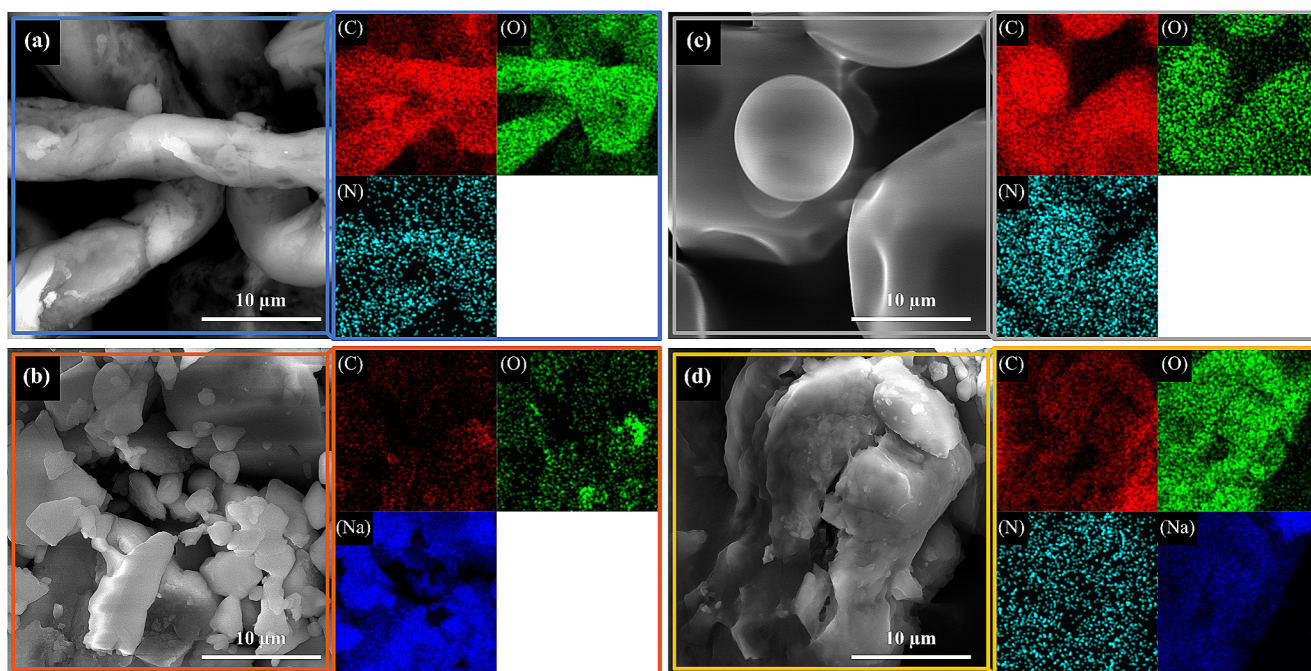


Fig. 3 FE-SEM images of (a) chitosan, (b) alginate, (c) PVP, and (d) CsAgPVP

study showed that the best removal efficiency was obtained in an acidic environment. At low pH (pH=3 and 4), the removal percentage reached more than 90%. The dominant form of Cr(VI) is HCrO_4^- , which has acidic properties. Increasing the adsorption of Cr(VI) in acidic media is due to the electrostatic attraction force between the positively charged surface of CsAgPVP and HCrO_4^- . The surface becomes negative at higher pH (pH=>5), making it difficult to adsorb HCrO_4^- [5]. CsAgPVP was difficult to adsorb HCrO_4^- at pH=>5 because neutral and alkaline pH causes CsAgPVP to become aggressive [25]. At pH=>5, the chains on the surface of CsAgPVP are accreted by deprotonation of the amine groups [26]. The adsorption test showed an optimum pH of 4.

3.3 Adsorption isotherm and kinetic

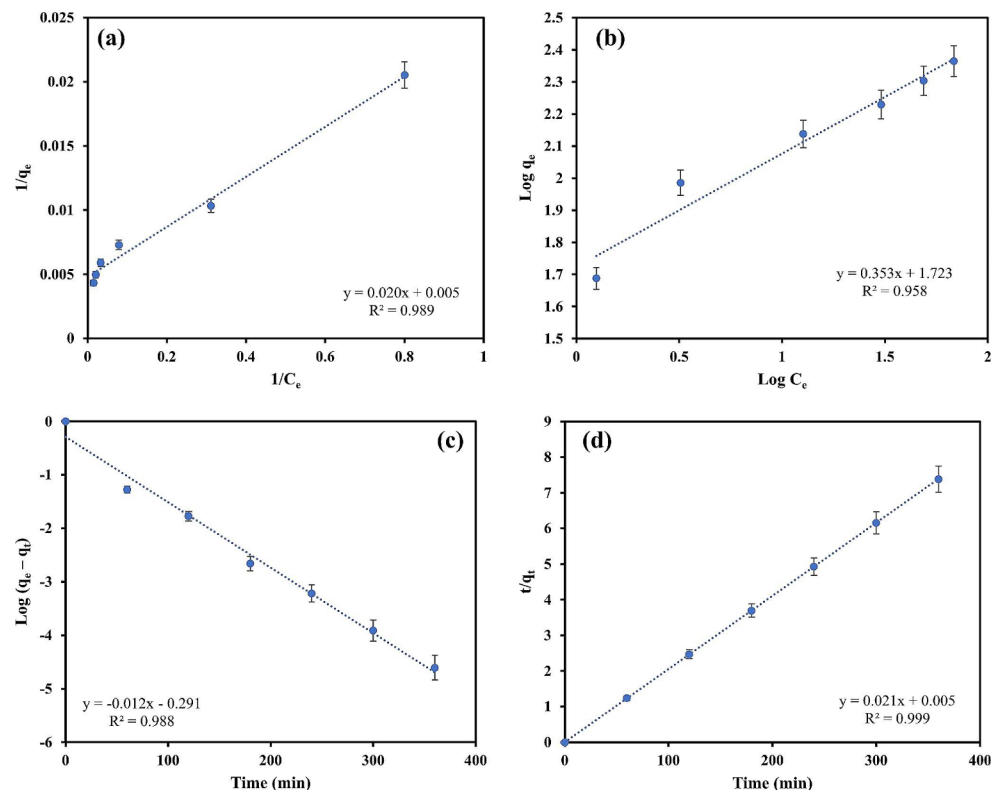
The next adsorption study is to determine the adsorption isotherm and kinetic values. In adsorption isotherms and kinetics, a process, type, and mechanism of adsorption are always used [27]. Understanding the interactions on the adsorbent and studying the improvement of adsorption performance is an important value. Adsorption isotherms generally use Langmuir and Freundlich model. Kinetic adsorption generally uses pseudo-first-order and pseudo-second-order.

The graph of the lineal equation used for the Cr(VI) adsorption study can be seen in Fig. 5a-b, and the isotherm parameters can be seen in Table S1. The Langmuir isotherm

assumes that the adsorption process is homogeneous. In contrast, the Freundlich isotherm assumes that the adsorption process is heterogeneous. By determining the R^2 value, it is obtained that the adsorption of Cr(VI) is Langmuir or Freundlich. The R^2 value of langmuir ($R^2=0.98$) is higher than freundlich ($R^2=0.95$). It indicates that the adsorption isotherm that occurs is the Langmuir. It can be assumed that the adsorption process is homogeneous. The adsorption capacity value obtained is 208.67 mg/g.

The linear equation graph of Cr(VI) adsorption kinetics can be seen in Fig. 6c-d, and the kinetic parameters can be seen in Table S2. The pseudo-first-order and pseudo-second-order kinetic models determined the adsorption uptake against time [28]. It was also used to determine the constant concentration. It is also used to determine the adsorbate diffusion in the adsorbent pore. Pseudo-first-order assumed that physisorption increases the adsorption rate of particles onto the adsorbent. In contrast, pseudo-second-order assumed chemisorption on the rate-limiting mechanism of the process. Determining the R^2 value of the kinetics can determine a pseudo-first-order or pseudo-second-order adsorption process. The R^2 value of pseudo-second-order ($R^2=0.99$) is higher than pseudo-first-order ($R^2=0.98$). It indicates that the kinetic adsorption that occurs is pseudo-second-order. The adsorption of Cr(VI) is caused by the electrostatic attraction between the positively charged amino ($-\text{NH}_3^+$) on the adsorbent surface and the negatively charged chromate (HCrO_4^-) [29, 30].

Fig. 5 The adsorption of Cr(VI) onto CsAgPVP of (a) Langmuir and (b) Freundlich isotherm model. Kinetics plots for removal of Cr(VI) by CsAgPVP of (c) pseudo-first-order and (d) pseudo-second-order



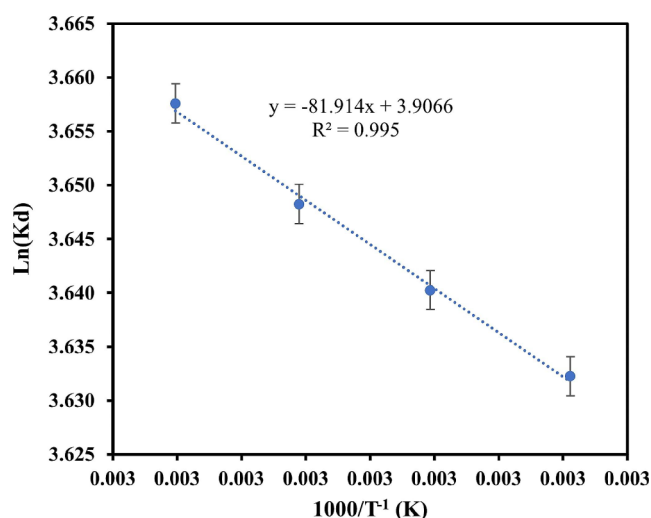


Fig. 6 Effect of temperature to adsorption

Table 2 Cr(VI) adsorption performance with other chitosan-based adsorbents

No	Adsorbent	pH	Adsorption capacity (mg/g)	Reference
1	Diethylenetriaminepentaacetic acid-thiourea- modified magnetic chitosan	4	122.03	[31]
2	Chitosan/cellulose nanocrystals grafted with carbon dots	2	217.8	[32]
3	Chitosan-pyrazoloquinoxaline	6	117.6	[33]
4	Chitosan/fly ash	5	33.27	[34]
5	FeS/chitosan/biochar	2	103.93	[35]
6	Fe(III)-chitosan microbeads	3	34.15	[36]
7	CsAgPVP	4	208.67	This study

A comparison of Cr(VI) adsorption using chitosan-based adsorbents can be seen in Table 2. The adsorption capacity obtained using CsAgPVP has a high value and is not much different from other chitosan-based adsorbents. It shows feasibility and applicability as a practical solution for Cr(VI) adsorption.

3.4 Adsorption thermodynamic

The thermodynamic parameters used in adsorption are Gibbs free energy (ΔG°) due to the transfer of one solute molecule from solution to solid/liquid surface area, enthalpy of adsorption (ΔH°), and entropy of adsorption (ΔS°). Equilibrium isotherm parameters can be seen in Table S3. The ΔH° shows a positive value of 0.68 kJ/mol. It indicates that the Cr(VI) adsorption process is endothermic. The endothermic nature confirms an increase in retention as the temperature of the solution increases, as seen in Fig. 7. The value of ΔS° is 0.03 kJ/mol.K, which shows a positive value. It

indicates a good affinity of the adsorbent towards Cr(VI) ions. In addition, it reflects an increase in the disorder factor at the solid/solution interface with some possible structural changes in the adsorbent during the adsorption process. The ΔG° values at 298 K, 308 K, 318 K, and 328 K are -9.00 kJ/mol, -9.32 kJ/mol, -9.65 kJ/mol, and -9.97 kJ/mol. The ΔG° value is negative, which indicates that the adsorption process is spontaneous [5, 37].

3.5 Exploration of the adsorption mechanism

FTIR spectra of CsAgPVP after adsorption of Cr(VI) can be seen in Fig. 6a. The after-adsorption FTIR spectrum shows the functional groups involved in the adsorption process. CsAgPVP before adsorption shows a peak at 3300 cm^{-1} , but there is a shift after adsorption to 3380 cm^{-1} . It indicates that the -OH group is involved in adsorption. A new peak was observed after Cr(VI) adsorption at 1056 cm^{-1} . There is a peak shift before and after adsorption, namely 1590 cm^{-1} to 1595 cm^{-1} . It indicates that the -C=O group is involved in the adsorption process. The -COOH group is also involved in adsorption due to the shift after Cr(VI) adsorption to 1417 cm^{-1} . FE-SEM images of CsAgPVP after Cr(VI) adsorption can be seen in Fig. 6b. The SEM images show a spherical surface on the surface of CsAgPVP. The spherical shape is typical of Cr [38, 39]. It indicates that Cr(VI) has been adsorbed to the surface of CsAgPVP. The FE-SEM images also show the presence of Cr.

3.6 Regeneration study

A graph of the regeneration potential of CsAgPVP at six cycles can be seen in Fig. 8. CsAgPVP that had adsorbed Cr(VI) was refined using NaOH. In the first to fourth cycles, the adsorption removal can still survive at 90%. However, in the fifth cycle, the removal percentage will decrease to 75%. Likewise, the sixth cycle removal percentage reached 49%. CsAgPVP can be used up to 4 times regeneration with a removal percentage reaching 90%.

3.7 Application on mine wastewater and waste acid laboratory

The CsAgPVP adsorbent study applied to real samples of mine wastewater and laboratory acid waste can be seen in Fig. 9. The removal percentages of Cr(VI) obtained in mine wastewater and laboratory acid waste were 80% and 72%. The removal percentage decreased when compared to the aqueous solution. It happens because of the competition between pollutants in the real sample [40, 41]. The almost limited decrease in Cr(VI) adsorption ability can

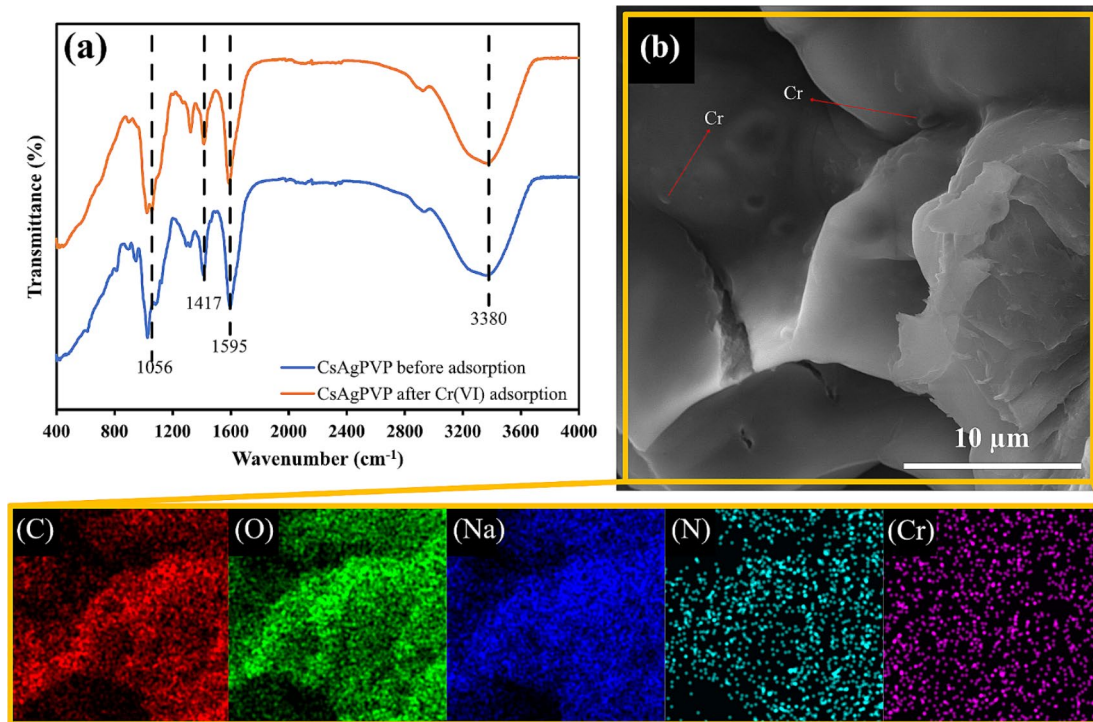


Fig. 7 Characterization CsAgPVP after adsorption Cr(VI) of (a) FTIR spectra and (b) FE-SEM images

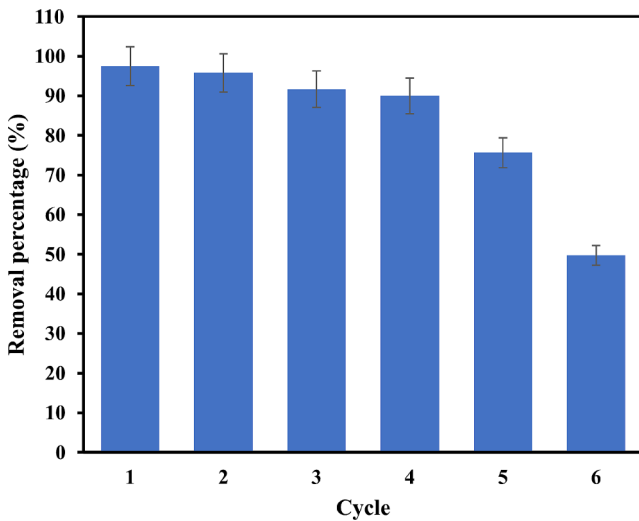


Fig. 8 Regeneration study of CsAgPVP up to 6 cycles. Experimental study: contact time=60 min; adsorbent amount=1 g/L; concentration=50 ppm; pH=4

be explained by the resistance of other ions in the aqueous medium.

4 Conclusions

Synthesis of CsAgPVP has been carried out. FTIR spectra show peaks at 1415 cm^{-1} , 1323 cm^{-1} , 1029 cm^{-1} , and 448 cm^{-1} , which are COO, C-N, C-O, and N-C=O groups.

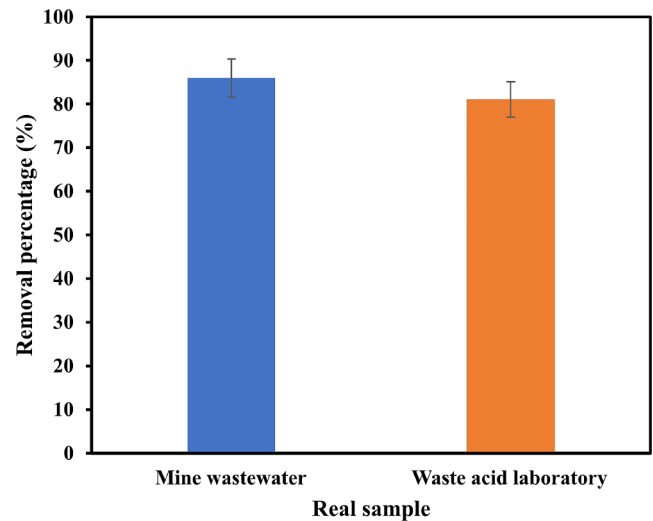


Fig. 9 Effect of heavy metal adsorption using adsorbent CsAgPVP on mine wastewater and acid laboratory. Experimental study: contact time=360 min; adsorbent amount=1 g/L

The surface area of CsAgPVP was 20.42 m^2/g . The pore size of CsAgPVP was 5.36 nm. Field emission shows the C, O, N, and Na. The optimum conditions CsAgPVP for adsorption Cr(VI) were 50 ppm, 360 min, and pH 4. It uses adsorption isotherm and kinetic to show the Langmuir model and pseudo-second-order. The CsAgPVP adsorption process is assumed homogeneous and considered as chemisorption. Adsorption capacity shows 208.67 mg/g. It uses a

regeneration study of removal percentage up to 90% in the fourth cycle. The removal percentage in real sample mine wastewater and waste acid laboratories was 80% and 72%.

Supplementary Information The online version contains supplementary material available at <https://doi.org/10.1007/s10450-024-00521-3>.

Acknowledgements This study was supported by the National Research and Innovation Agency (BRIN).

Author contributions Amru Daulay: Methodology, Conceptualization, Writing—original draft, Reviewing and Editing; David Candra Birawidha: Methodology, Data curation, Writing—original draft; Singgih Prabowo: Conceptualization, Writing, Reviewing and Editing; Evi Dwi Yanti: Conceptualization, Writing, Reviewing and Editing; Lukman Hakim Nasution: Conceptualization, Writing, Reviewing and Editing; Lukmanul Hakim Samada, Reviewing and Editing.

Funding This study was funded by the National Research and Innovation Agency (BRIN) with grant number B-1484/III.10/TK.01.00/2/2024.

Data availability No datasets were generated or analysed during the current study.

Declarations

Ethical approval No animal or humans were used in this research.

Competing interests The authors declare no competing interests.

References

- Szakli, E.: Human Health effects of oral exposure to Chromium: A systematic review of the Epidemiological evidence. *Int. J. Environ. Res. Public. Health.* **21**, 406 (2024). <https://doi.org/10.3390/ijerph21040406>
- Wise, J.P., Young, J.L., Cai, J., Cai, L.: Current understanding of hexavalent chromium [Cr(VI)] neurotoxicity and new perspectives. *Environ. Int.* **158**, 106877 (2022). <https://doi.org/10.1016/j.envint.2021.106877>
- Dhal, B., Das, N.N., Thatoi, H.N., Pandey, B.D.: Characterizing toxic cr(VI) contamination in chromite mine overburden dump and its bacterial remediation. *J. Hazard. Mater.* **260**, 141–149 (2013). <https://doi.org/10.1016/j.jhazmat.2013.04.050>
- Prasad, S., Yadav, K.K., Kumar, S., Gupta, N., Cabral-Pinto, M.M.S., Rezanian, S., Radwan, N., Alam, J.: Chromium contamination and effect on environmental health and its remediation: A sustainable approaches. *J. Environ. Manage.* **285**, 112174 (2021). <https://doi.org/10.1016/j.jenvman.2021.112174>
- Alqarni, L.S., Algethami, J.S., Kaim Billah, E.L., Alorabi, R., Alnaam, A.Q., Algethami, Y.A., Bahsis, F.K., Jawad, L., Wasilewska, A.H., López-Maldonado, M.: A novel chitosan-alginate@Fe/Mn mixed oxide nanocomposite for highly efficient removal of cr (VI) from wastewater: Experiment and adsorption mechanism. *Int. J. Biol. Macromol.* **263**, 129989 (2024). <https://doi.org/10.1016/j.ijbiomac.2024.129989>
- Sheth, Y., Dharaskar, S., Khalid, M., Walvekar, R.: Investigating chromium cr(VI) removal using imidazolium based ionic liquid-chitosan composite adsorptive film. *J. Mol. Liq.* **347**, 118317 (2022). <https://doi.org/10.1016/j.molliq.2021.118317>
- Qasem, N.A.A., Mohammed, R.H., Lawal, D.U.: Removal of heavy metal ions from wastewater: A comprehensive and critical review. *npj Clean. Water.* **4**, 36 (2021). <https://doi.org/10.1038/s41545-021-00127-0>
- Mehrizad, A.: Adsorption studies of some phenol derivatives onto Ag-cuttlebone nanobiocomposite: Modeling of process by response surface methodology. *Res. Chem. Intermed.* **43**, 4295–4310 (2017). <https://doi.org/10.1007/s11164-017-2874-y>
- Rajendran, S., Priya, A.K., Senthil Kumar, P., Hoang, T.K.A., Sekar, K., Chong, K.Y., Khoo, K.S., Ng, H.S., Show, P.L.: A critical and recent developments on adsorption technique for removal of heavy metals from wastewater-A review. *Chemosphere.* **303**, 135146 (2022). <https://doi.org/10.1016/j.chemosphere.2022.135146>
- Mehrizad, A., Aghaie, M., Gharbani, P., Dastmalchi, S., Monajjemi, M., Zare, K.: Comparison of 4-chloro-2-nitrophenol adsorption on single-walled and multi-walled carbon nanotubes. *Iran. J. Environ. Health Sci. Eng.* **9**, 5 (2012). <https://doi.org/10.1186/1735-2746-9-5>
- Hassanzadeh, P., Gharbani, P., Derakhshanfard, F., Memar Maher, B.: Preparation and characterization of PVDF/g-C3N4/Chitosan Polymeric Membrane for the removal of direct blue 14 dye. *J. Polym. Environ.* **29**, 3693–3702 (2021). <https://doi.org/10.1007/s10924-021-02145-y>
- Argüelles-Monal, W., Lizardi-Mendoza, J., Fernández-Quiroz, D., Recillas-Mota, M., Montiel-Herrera, M.: Chitosan Derivatives: Introducing New functionalities with a controlled Molecular Architecture for innovative materials. *Polym. (Basel)*. **10**, 342 (2018). <https://doi.org/10.3390/polym10030342>
- Guo, H., Qin, Q., Chang, J.-S., Lee, D.-J.: Modified alginate materials for wastewater treatment: Application prospects. *Bioresour Technol.* **387**, 129639 (2023). <https://doi.org/10.1016/j.biortech.2023.129639>
- Yu, S., Yang, Y., Kuroda, K., Pu, J., Guo, R., Hou, L.-A.: Selective removal of cr(VI) using polyvinylpyrrolidone and polyacrylamide co-modified MoS2 composites by adsorption combined with reduction. *Chin. Chem. Lett.* **35**, 109130 (2024). <https://doi.org/10.1016/j.ccllet.2023.109130>
- Afriani, K., Sutanti Budikania, T.: Synthesis and characterization of Hydrogel of Chitosan-Poly (N-Vinyl-2-Pyrrolidone) (PVP)-Alginate for Ibuprofen Release. *J. Pure Appl. Chem. Res.* **9**, 201–211 (2020). <https://doi.org/10.21776/ub.jpacr.2020.009.03.558>
- Hadjiivanov, K.I., Panayotov, D.A., Mihaylov, M.Y., Ivanova, E.Z., Chakarova, K.K., Andonova, S.M., Drenchev, N.L.: Power of Infrared and Raman Spectroscopies to Characterize Metal-Organic frameworks and investigate their Interaction with Guest molecules. *Chem. Rev.* **121**, 1286–1424 (2021). <https://doi.org/10.1021/acs.chemrev.0c00487>
- Nadour, M., Boukraa, F., Ouradi, A., Benaboura, A.: Effects of Methylcellulose on the properties and morphology of polysulfone membranes prepared by phase inversion. *Mater. Res.* **20**, 339–348 (2017). <https://doi.org/10.1590/1980-5373-mr-2016-0544>
- Alqutaibi, A.Y., Baik, A., Almuzaini, S.A., Farghal, A.E., Alnazawi, A.A., Borzangy, S., Aboalrejal, A.N., AbdElaziz, M.H., Mahmoud, I.I., Zafar, M.S.: Polymeric denture base materials: A review. *Polym. (Basel)*. **15**, 3258 (2023). <https://doi.org/10.3390/polym15153258>
- Saba, N., Jawaid, M.: A review on thermomechanical properties of polymers and fibers reinforced polymer composites. *J. Ind. Eng. Chem.* **67**, 1–11 (2018). <https://doi.org/10.1016/j.jiec.2018.06.018>
- You, R., Xiao, C., Zhang, L., Dong, Y.: Versatile particles from water-soluble chitosan and sodium alginate for loading toxic or

- bioactive substance. *Int. J. Biol. Macromol.* **79**, 498–503 (2015). <https://doi.org/10.1016/j.ijbiomac.2015.05.025>
21. Purohit, P., Bhatt, A., Mittal, R.K., Abdellatif, M.H., Farghaly, T.A.: Polymer grafting and its chemical reactions. *Front. Bioeng. Biotechnol.* **10** (2023). <https://doi.org/10.3389/fbioe.2022.1044927>
 22. Krasnoselskaya, I.G., Turkova, L.D., Baranovskaya, I.A., Klenin, S.I., Erusalimskii, B.L.: Synthesis and study of grafted polymers formed on interaction of polyacrylonitrile live chains with polyvinylpyridines. *Polym. Sci. U S S R.* **32**, 928–933 (1990). [https://doi.org/10.1016/0032-3950\(90\)90227-W](https://doi.org/10.1016/0032-3950(90)90227-W)
 23. Xue, F., He, H., Zhou, H., Quan, Z., Chen, Z., Wu, Q., Zhu, H., Wang, S.: Structural design of a cellulose-based hyperbranched adsorbent for the rapid and complete removal of Cr(VI) from water. *Chem. Eng. J.* **417**, 128037 (2021). <https://doi.org/10.1016/j.cej.2020.128037>
 24. Li, L., Liu, F., Duan, H., Wang, X., Li, J., Wang, Y., Luo, C.: The preparation of novel adsorbent materials with efficient adsorption performance for both chromium and methylene blue. *Colloids Surf. B Biointerfaces.* **141**, 253–259 (2016). <https://doi.org/10.1016/j.colsurfb.2015.06.023>
 25. Athavale, R., Sapre, N., Rale, V., Tongaonkar, S., Manna, G., Kulkarni, A., Shirolkar, M.M.: Tuning the surface charge properties of chitosan nanoparticles. *Mater. Lett.* **308**, 131114 (2022). <https://doi.org/10.1016/j.matlet.2021.131114>
 26. Kim, H.-S., Lee, S.-H., Eun, C.-J., Yoo, J., Seo, Y.-S.: Dispersion of chitosan nanoparticles stable over a wide pH range by adsorption of polyglycerol monostearate. *Nanomater Nanotechnol.* **10**, 184798042091726 (2020). <https://doi.org/10.1177/1847980420917260>
 27. Andriyani, M., Suharman, Daulay, A.: Synthesis of mesoporous silica with ricinoleic methyl ester (*Ricinus communis*) as a template for adsorption copper (II) with optimizing Box-Behnken design. *Case Stud. Chem. Environ. Eng.* **7**, 100287 (2023). <https://doi.org/10.1016/j.csee.2022.100287>
 28. Revellame, E.D., Fortela, D.L., Sharp, W., Hernandez, R., Zappi, M.E.: Adsorption kinetic modeling using pseudo-first order and pseudo-second order rate laws: A review. *Clean. Eng. Technol.* **1**, 100032 (2020). <https://doi.org/10.1016/j.clet.2020.100032>
 29. Khalil, T.E., Abdel-Salam, A.H., Mohamed, L.A., El-Meligy, E., El-Dissouky, A.: Crosslinked modified chitosan biopolymer for enhanced removal of toxic Cr(VI) from aqueous solution. *Int. J. Biol. Macromol.* **234**, 123719 (2023). <https://doi.org/10.1016/j.ijbiomac.2023.123719>
 30. Long, W., Chen, Z., Chen, X., Zhong, Z.: Investigation of the Adsorption process of chromium (VI) ions from Petrochemical Wastewater using Nanomagnetic Carbon materials. *Nanomaterials.* **12**, 3815 (2022). <https://doi.org/10.3390/nano12213815>
 31. Zhang, B., Hu, R., Sun, D., Wu, T., Li, Y.: Fabrication of chitosan/magnetite-graphene oxide composites as a novel bioadsorbent for adsorption and detoxification of Cr(VI) from aqueous solution. *Sci. Rep.* **8**, 15397 (2018). <https://doi.org/10.1038/s41598-018-33925-7>
 32. Zeng, H., Hu, Z., Peng, C., Deng, L., Liu, S.: Effective adsorption and sensitive detection of Cr(VI) by Chitosan/Cellulose nanocrystals grafted with Carbon dots Composite Hydrogel. *Polym. (Basel).* **13**, 3788 (2021). <https://doi.org/10.3390/polym13213788>
 33. Elhag, M., Abdelwahab, H.E., Mostafa, M.A., Nasr, A.Z., El Sadek, M.M.: Synthesis and characterization of chitosan-pyrazoloquinoline Schiff bases for Cr(VI) removal from wastewater. *Int. J. Biol. Macromol.* **163**, 2180–2188 (2020). <https://doi.org/10.1016/j.ijbiomac.2020.09.090>
 34. Wen, Y., Tang, Z., Chen, Y., Gu, Y.: Adsorption of Cr(VI) from aqueous solutions using chitosan-coated fly ash composite as biosorbent. *Chem. Eng. J.* **175**, 110–116 (2011). <https://doi.org/10.1016/j.cej.2011.09.066>
 35. Yang, Y., Zhang, Y., Wang, G., Yang, Z., Xian, J., Yang, Y., Li, T., Pu, Y., Jia, Y., Li, Y., Cheng, Z., Zhang, S., Xu, X.: Adsorption and reduction of Cr(VI) by a novel nanoscale FeS/chitosan/biochar composite from aqueous solution. *J. Environ. Chem. Eng.* **9**, 105407 (2021). <https://doi.org/10.1016/j.jece.2021.105407>
 36. Tandekar, S.A., Pande, M.A., Shekhawat, A., Fosso-Kankeu, E., Pandey, S., Jugade, R.M.: Fe(III)-Chitosan Microbeads for Adsorptive removal of Cr(VI) and phosphate ions. *Minerals.* **12**, 874 (2022). <https://doi.org/10.3390/min12070874>
 37. Kaim Billah, E.L., Zaghoul, R., Bahsis, A., Oladoja, L., Azoubi, N.A., Taoufyk, Z., Majdoubi, A., Algethami, H., Soufiane, J.S., López-Maldonado, A., Wasilewska, E.A., Elboughdiri, M.: Multifunctional biocomposites based on cross-linked shrimp waste-derived chitosan modified Zn₂+@Calcium apatite for the removal of methyl orange and antibacterial activity. *Mater. Today Sustain.* **25**, 100660 (2024). <https://doi.org/10.1016/j.mtsust.2023.100660>
 38. Leimbach, M., Tschaar, C., Zapf, D., Kurniawan, M., Schmidt, U., Bund, A.: Relation between Color and Surface morphology of Electrodeposited Chromium for decorative applications. *J. Electrochem. Soc.* **166**, D205–D211 (2019). <https://doi.org/10.1149/2.0871906jes>
 39. Protsenko, V.S., Gordiienko, V.O., Danilov, F.I., Kwon, S.C.: Preparation and characterization of Nanocrystalline Hard Chromium Coatings using eco-friendly trivalent chromium bath. *E-J. Chem.* **8**, 1925–1929 (2011). <https://doi.org/10.1155/2011/253203>
 40. Chen, Y.-G., He, Y., Ye, W.-M., Jia, L.-Y.: Competitive adsorption characteristics of Na(I)/Cr(III) and Cu(II)/Cr(III) on GMZ bentonite in their binary solution. *J. Ind. Eng. Chem.* **26**, 335–339 (2015). <https://doi.org/10.1016/j.jiec.2014.12.006>
 41. Quintáns-Fondo, A., Ferreira-Coelho, G., Arias-Estévez, M., Nóvoa-Muñoz, J.C., Fernández-Calviño, D., Álvarez-Rodríguez, E., Fernández-Sanjurjo, M.J., Núñez-Delgado, A.: Chromium VI and fluoride competitive adsorption on different soils and By-Products. *Processes.* **7**, 748 (2019). <https://doi.org/10.3390/pr7100748>

Publisher's Note Springer Nature remains neutral with regard to jurisdictional claims in published maps and institutional affiliations.

Springer Nature or its licensor (e.g. a society or other partner) holds exclusive rights to this article under a publishing agreement with the author(s) or other rightsholder(s); author self-archiving of the accepted manuscript version of this article is solely governed by the terms of such publishing agreement and applicable law.